

An Integrated Multi-Port Driven Radiating Source

Steven M. Bowers and Ali Hajimiri
California Institute of Technology, Pasadena, California, 91125, USA

Abstract—A multi-port driven (MPD) antenna allows for the removal of RF blocks for impedance matching, power combining, and power delivery by enabling efficient radiation at the fundamental frequency from several output stages driving the antenna. A radiating source utilizing an 8-phase ring oscillator and eight power amplifiers to drive the MPD antenna at 161 GHz with a total radiated power of -2 dBm and a single element EIRP of 4.6 dBm is demonstrated in silicon with single lobe radiation patterns closely matching simulation.

Index Terms—Antennas, Millimeter wave integrated circuits, Antenna radiation patterns, Integrated Antenna, BiCMOS

I. INTRODUCTION

The many potential applications at mm-wave frequencies combined with our ability to integrate a large number of high-speed transistors present an opportunity to investigate novel power generation and radiation architectures in silicon-based integrated circuits. However, integrated power generation, and in particular, radiation bring up several challenges ranging from on-chip power combining and impedance matching to off-chip power transfer. The traditional power transfer methods (e.g., bonding wires and solder balls) to off-chip loads (e.g., external antenna) also become increasingly challenging.

At the same time, the smaller wavelengths associated with these frequencies opens up the possibility of radiating the power directly from the chip itself, rather than losing significant power by electrically connecting to an off-chip antenna [1] - [5]. The low breakdown voltages of integrated silicon transistors encourages the use of large or highly parallel transistors for high power generation, leading to low optimal load impedances from the active drivers perspective. Unfortunately, this directly conflicts with single-port antenna impedance level trade-offs, where a large radiation resistance compared to the loss resistance is preferred for high efficiency.

The ability to implement complex structures on silicon chips combined with the high frequency capabilities of the transistors widens the available design space considerably. This enables an integrated Multi-Port Driven (MPD) antenna, which is an antenna that is driven at the fundamental radiating frequency at many points with different signals. Such MPD antennas can be used to overcome the trade-offs between the port impedance and antenna efficiency due to energy losses in the antenna. With careful design, taking advantage of the current superposition of many driving sources, low input impedance can be achieved directly at the antenna port while keeping the radiation efficiency high. This eliminates the need for internal matching networks between the active drivers and the on-chip antenna, resulting in additional energy loss. An added advantage of the MPD structure is its intrinsic power

combining capability, where local current combining results in far field power combining. This is particularly conducive to silicon integrated power generation. Thus, an MPD antenna provides an efficient way to transfer and radiate power off chip, while concurrently performing impedance matching and power combining.

II. MPD ANTENNA DESIGN

To produce efficient radiation from a chip, the integration of RF current density across the entire chip needs to add coherently, and produce electromagnetic fields that similarly will add constructively in the far field due to superposition. One way to achieve such a current density distribution is to create a traveling wave current around a loop of similar circumference to the RF wavelength to produce a circular polarization [1], [2]. In this design, the traveling wave is created by driving the ring at the fundamental frequency, as shown in Fig. 1. Opposite sides of the ring will have maximum instantaneous currents at the same time that are 180° out of phase due to delay around the ring. However, the current vector is rotated another 180° due to the curvature of the ring, thus both current vectors add up constructively. In a radial MPD antenna, the core driving circuitry is placed at the center of the ring, and ‘spokes’ provide a return path for the ground current to maximize radiation. The ground plane of the chip is also pulled back away from the ring to ensure that the ground path going out the spokes to the ground plane has a much higher impedance than the path going down the spokes to the center of the radiator. These spokes are oriented perpendicular to the ring, and thus the fields produced by the ground current will be orthogonal to the fields produced by ground currents in the signal ring. In addition, there is a delay causing about a 45°

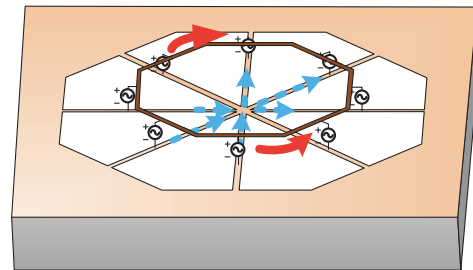


Fig. 1. Instantaneous current distribution on a radial multi-port driven (MPD) antenna, with red solid lines showing traveling wave signal current around the ring, and blue dashed lines showing standing wave ground current through the spokes.

phase shift between the current injected into the ring, and the maximum of the current traveling around the ring, that cause the fields created by ground currents within the ring and signal currents around the ring to add primarily constructively.

By symmetry, there is a virtual short at the center of the radiator, which creates standing waves along the ground spokes. Because each of the standing waves is phased evenly around the radiator, the ground currents still create circularly polarized radiation, similar to two orthogonal dipoles in quadrature. The silicon substrate has a relative permittivity of 11.7, causing most of the power to be radiated down into the substrate. While it is possible to radiate out of the backside of the chip this way, due to the practical thermal and packaging concerns, it is preferable to radiate from the top side by mounting the chip on a conductive backplane about $1/4$ wavelength from the antenna. The electromagnetic waves experience a 90° phase shift down to the backplane, a 180° phase shift on the reflection, and a 90° phase shift traveling back up to the top of the chip, for a 360° total phase shift, and thus will add constructively with the fields that are directly radiated up.

In order to create the traveling wave on the ring, at least three drives are required, but for practical design purposes powers of two are preferable for the number of spokes. The ground spokes also provide shielding for feed lines that connect the oscillator and amplifier core out to the ring by providing a closed path for the return current.

An 8-spoke proof of concept MPD radiating source consisting of active drive circuitry and a circular MPD antenna operating at 160 GHz was designed and fabricated in a 130 nm SiGe BiCMOS process with two $3 \mu\text{m}$ copper top metal layers. The MPD antenna has a simulated radiation efficiency of 24%, and directivity of 8.8 dB, yielding a gain of 2.5 dBi, and a maximum equivalent isotropic radiated power (EIRP) of 4.5 dBm at 160 GHz. The antenna gain is simulated to have a variation of less than 1 dB from 140 GHz to 165 GHz.

III. CIRCUIT DESIGN

To prevent coupling from any external sources back to the oscillator, a unilaterally driven design from the oscillator to the antenna is desired. This is achieved by separating the reactive elements of the oscillator from those on the antenna, and placing an amplification stage between the oscillator and antenna. The block diagram of the radiator is shown in Fig. 2.

The total area available within the center of the radiator is small, and thus it is preferable to employ a power oscillator to provide sufficient power directly. A single amplifying stage is used next to amplify the signal and provide reverse isolation between the radiator and oscillator. The central oscillator is a 4-stage differential ring oscillator that provides eight phases separated by 45° , with Fig. 3 showing its schematic.

Each amplifier is a cascode stage for increased power and voltage swing, and employs tuned metal capacitors for AC-coupling of the stages. The results of [6] are used to determine the interstage connections of the oscillator. Each of the eight oscillator phases is then fed to a cascode amplifying stage, which provides 6 dB gain and -7 dBm output power at 160

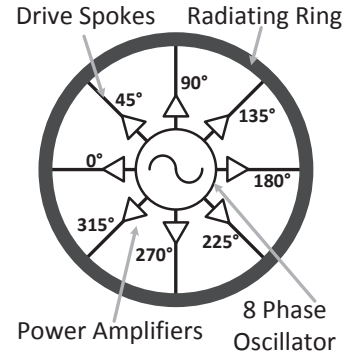


Fig. 2. Block diagram of the multi-port driven (MPD) radiator.

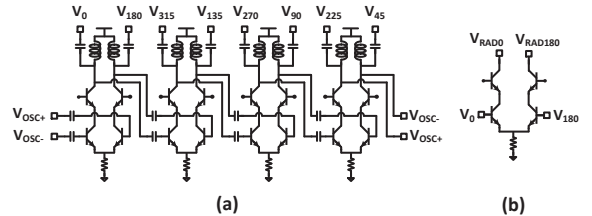


Fig. 3. Circuit schematics of the 8 phase ring oscillator (a), and the power amplifier at the output of each stage (b). Biasing circuitry omitted for simplicity.

GHz each in simulation for a total simulated output power of 2 dBm, as seen in Fig. 3.

IV. MEASUREMENTS

The chip was thinned to around $190 \mu\text{m}$, mounted on a PCB, and attached to a 2-D stepper motor setup to measure the antenna pattern, without any other post-processing steps or external silicon lenses. It was measured using a receiver consisting of a 23.4 dB gain linearly polarized horn antenna and a 10th harmonic WR-6 mixer fed into a spectrum analyzer. The receiver was calibrated using a 160 GHz tripler source and an Erikson power meter. All measurements were taken with a separation of 75 mm, or 40λ at 160 GHz. The chip was rotated in the X-Y plane and confirmed to have circular polarization. The radiator was measured to have a maximum 4.6 dBm EIRP, at a frequency of 161.45 GHz while dissipating 384 mW, in close agreement with simulation. The calibrated power spectrum of the receiver is depicted in Fig. 4. The radiation pattern was measured, and shows a total radiated output power of -2 dBm. Two perpendicular slices of the radiation pattern are presented in Fig. 5.

Because of the limited tuning range of the 160 GHz oscillator, the oscillator inductors were designed to be laser trimmable, allowing for two additional lower frequency bands. This was used to verify the bandwidth of the antenna itself. Measurements of EIRP for all three frequency bands and simulated gain from 140 to 165 GHz are shown in Fig. 6. Tuning within each frequency band is performed through bias control, though the output power of the oscillator suffers the

TABLE I
COMPARISON OF INTEGRATED RADIATING SOURCES IN SILICON ABOVE 100 GHz.

Reference	Frequency	Total Radiated Power	Maximum EIRP	Process	Number of Elements	DC Power Consumption
This Work	161 GHz	-2.0 dBm	4.6 dBm	130 nm SiGe	1	386 mW
[1]	191 GHz	-12.4 dBm	-1.9 dBm	65 nm CMOS	4	77 mW
[2]	280 GHz	-7.2 dBm	9.4 dBm	45 nm CMOS SOI	16	817 mW
[3]	165 GHz	-27 dBm	N/A	130 nm SiGe	1	800 mW (full transceiver)
[4]	144 GHz	N/A	<0.1 dBm	65 nm CMOS	1	219 mW
[5]	380 GHz	N/A	-13 dBm	130 nm SiGe	2	364 mW (full transceiver)

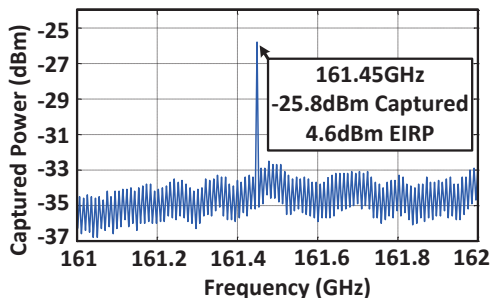


Fig. 4. Calibrated measured spectrum of the multi-port driven (MPD) radiator.

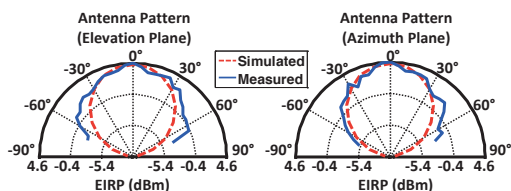


Fig. 5. Simulated and measured radiation pattern in both the elevation and azimuth planes.

further the bias is from the ideal operating point. Because simulations show that the antenna gain is near constant across the frequency range, the decrease in EIRP for the two lower bands is attributed to impedance mismatch in the interstage match of the oscillator stages as well as between the oscillator and amplifiers, causing the available power to the antenna to be lower in those bands. A comparison against other on-chip silicon radiating sources above 100 GHz is presented in Table I, and a die photo of the radiator is shown in Fig. 7.

V. CONCLUSION

This paper presents and verifies the viability of MPD antennas and radiating sources. Improvements in power transfer, impedance matching and power combining achieved using MPD antennas enable radiated power measurements of -2 dBm with a measured EIRP of 4.6 dBm at 161GHz.

ACKNOWLEDGMENT

The authors would like to thank ST Microelectronics for chip fabrication.

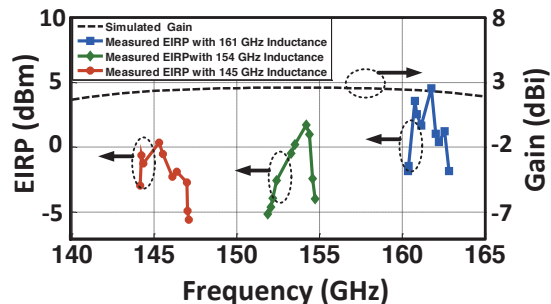


Fig. 6. Simulated gain across frequency of the multi-port driven (MPD) antenna and measured EIRP across three frequency bands that are created by laser trimming the oscillator inductors. Frequency tuning within each band is achieved through bias control at the expense of output power.

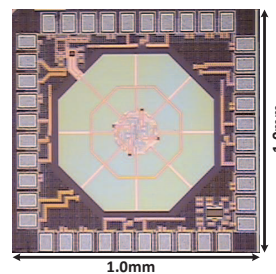


Fig. 7. Die photo of the MPD radiating source

REFERENCES

- [1] K. Sengupta and A. Hajimiri, "Sub-THz beam-forming using near-field coupling of Distributed Active Radiator arrays," *Radio Frequency Integrated Circuits Symposium (RFIC)*, June 2011.
- [2] K. Sengupta and A. Hajimiri, "A 0.28THz 4x4 power-generation and beam-steering array," *International Solid State Circuits Conference Digest (ISSCC)*, pp.256-258, Feb. 2012.
- [3] E. Laskin, et al., "170-GHz transceiver with on-chip antennas in SiGe technology," *Radio Frequency Integrated Circuits Symposium Digest (RFIC)*, pp.637-640, June 2008
- [4] A. Tang, et al., "A 144GHz 0.76cm-resolution sub-carrier SAR phase radar for 3D imaging in 65nm CMOS," *International Solid State Circuits Conference Digest (ISSCC)*, pp.264-266, Feb. 2012
- [5] J.D. Park, et al., "A 0.38THz fully integrated transceiver utilizing quadrature push-push circuitry," *Symp. on VLSI Circuits (VLSIC)*, pp.22-23, June 2011
- [6] O. Momeni and E. Afshari, "High Power Terahertz and Millimeter-Wave Oscillator Design: A Systematic Approach," *IEEE J. of Solid-State Circuits*, vol.46, no.3, pp.583-597, March 2011.